AIP | Review of Scientific Instruments

Using high-intensity laser-generated energetic protons to radiograph directly driven implosions

A. B. Zylstra, C. K. Li, H. G. Rinderknecht, F. H. Séguin, R. D. Petrasso et al.

Citation: Rev. Sci. Instrum. **83**, 013511 (2012); doi: 10.1063/1.3680110
View online: http://dx.doi.org/10.1063/1.3680110
View Table of Contents: http://rsi.aip.org/resource/1/RSINAK/v83/i1
Published by the American Institute of Physics.

Using high-intensity laser-generated energetic protons to radiograph directly driven implosions

A. B. Zylstra,[1,a)] C. K. Li,[1] H. G. Rinderknecht,[1] F. H. Séguin,[1] R. D. Petrasso,[1,b)] C. Stoeckl,[2] D. D. Meyerhofer,[2,c)] P. Nilson,[2] T. C. Sangster,[2] S. Le Pape,[3] A. Mackinnon,[3] and P. Patel[3]

[1]*Plasma Science and Fusion Center, Massachusetts Institute of Technology, Cambridge, Massachusetts 02139, USA*
[2]*Laboratory for Laser Energetics, University of Rochester, Rochester, New York 14623, USA*
[3]*Lawrence Livermore National Laboratory, Livermore, California 94550, USA*

(Received 17 June 2011; accepted 8 January 2012; published online 31 January 2012)

The recent development of petawatt-class lasers with kilojoule-picosecond pulses, such as OMEGA EP [L. Waxer *et al.*, Opt. Photonics News **16**, 30 (2005)], provides a new diagnostic capability to study inertial-confinement-fusion (ICF) and high-energy-density (HED) plasmas. Specifically, petawatt OMEGA EP pulses have been used to backlight OMEGA implosions with energetic proton beams generated through the target normal sheath acceleration (TNSA) mechanism. This allows time-resolved studies of the mass distribution and electromagnetic field structures in ICF and HED plasmas. This principle has been previously demonstrated using Vulcan to backlight six-beam implosions [A. J. Mackinnon *et al.*, Phys. Rev. Lett. **97**, 045001 (2006)]. The TNSA proton backlighter offers better spatial and temporal resolution but poorer spatial uniformity and energy resolution than previous D^3He fusion-based techniques [C. Li *et al.*, Rev. Sci. Instrum. **77**, 10E725 (2006)]. A target and the experimental design technique to mitigate potential problems in using TNSA backlighting to study full-energy implosions is discussed. The first proton radiographs of 60-beam spherical OMEGA implosions using the techniques discussed in this paper are presented. Sample radiographs and suggestions for troubleshooting failed radiography shots using TNSA backlighting are given, and future applications of this technique at OMEGA and the NIF are discussed. © *2012 American Institute of Physics*. [doi:10.1063/1.3680110]

I. INTRODUCTION

The inertial confinement fusion (ICF) program seeks to achieve fusion ignition and positive target energy gain in the laboratory. The basic challenge is to compress a spherical shell of deuterium and tritium such that the central gas becomes hot and dense enough to "spark" thermonuclear burn that propagates through the main high-density fuel. Ongoing experiments at the National Ignition Facility (NIF) (Ref. 1) will attempt to demonstrate thermonuclear ignition in the laboratory using the indirect-drive approach, with polar drive and advanced ignition experiments to follow. Understanding target physics is crucial to achieving ignition at the NIF in these experiments. The fundamental implosion physics can be thoroughly studied at smaller scale facilities, such as OMEGA (Ref. 2) and OMEGA Extended Performance (EP) (Ref. 3) at the University of Rochester's Laboratory for Laser Energetics, who are leading the polar drive and shock ignition efforts.[4–6]

A. Previous techniques

One successful technique for studies of ICF implosions has been radiography using either x rays[7,8] or charged particles; the latter will be the focus of this paper. Within the past several years short-pulse-generated proton radiography has been demonstrated by Mackinnon *et al.* for six-beam implosions on the Vulcan laser.[9] Backlighting full-energy OMEGA implosions, as demonstrated in this work, reveals filamentary electromagnetic (EM) field structures in the corona that were not observed by Mackinnon *et al.*,[9] but were observed by Rygg *et al.*[10] using a fusion-based charged-particle backlighter technique was developed at OMEGA.[11] This method uses 3 and 15 MeV protons (from DD and D^3He fusion), produced in a 80–130 ps burn with a typical source size of 40–50 μm FWHM. This technique has been successfully used to study direct-drive implosions,[10,12,13] indirect-drive implosions,[14–16] and electromagnetic fields in HED plasmas.[17–21]

B. Energetic proton production

It is well-known that the interaction of a high-intensity laser with matter can create energetic electrons and ions.[22,23] Relevant to this work is the target normal sheath acceleration (TNSA) mechanism[24] at laser intensities on the order of 10^{19} W/cm^2. During the initial laser interaction with a solid target electrons are accelerated to high energy, and propagate away from the target at nearly the speed of light, c. This sets up strong "sheath" electric fields, which can accelerate ions to high energy. Hydrocarbon contaminants

a)Electronic mail: zylstra@mit.edu.
b)Also visiting senior scientist at Laboratory for Laser Energetics, University of Rochester, Rochester, NY, USA.
c)Also at Departments of Mechanical Engineering and Physics and Astronomy, University of Rochester, Rochester, NY, USA.

on the target are known to cause the production of protons with energies up to 60 MeV.[25] Ion acceleration mechanisms, including TNSA, have been extensively studied experimentally[24–43] and computationally.[44–47] Other proposed applications for this technique include compact medical and research accelerators,[48] and proton fast ignition.[49]

C. Challenges and benefits of TNSA backlighting

An obvious use of these sheath-generated proton beams is as a backlighter for ICF and HED plasmas. This has been proposed and used in the literature,[50–53] first demonstrated for six-beam spherical implosions using Vulcan,[9] and recently in experiments on OMEGA EP.[54–56] Backlighting full-scale implosions at OMEGA or the NIF comes with a unique set of challenges and benefits for TNSA proton backlighting.

These challenges include designing the backlighter to ensure an adequate fluence and energy of backlighting protons. This requires compensating for several effects, such as x-ray cross talk, return current, and preplasma from the implosion.[57] The beam divergence, magnification required, and desired radiography time window require experimental optimization.

The benefits of TNSA proton backlighting over previous proton backlighting, i.e., with fusion-generated protons, are better temporal resolution (~10 ps versus ~100 ps), better spatial resolution (~10 μm versus 40–50 μm), and the ability to radiograph at several time steps during one implosion. Spatial and temporal resolution are quoted on the basis of previous TNSA proton production and radiography work in the literature.[35,51,58] Information on the spectral resolution is also available within these works. The fusion backlighter offers better energy resolution and spatial uniformity than the TNSA backlighter; which technique is optimal depends on the experiment.

This work focuses on solutions to the unique challenges in using TNSA backlighting for 60-beam OMEGA implosions, and presents the first radiographs of such implosions. The paper is organized as follows: Sec. II presents an overview of the facilities and the experiment; Sec. III details the specifics of our backlighter design; Sec. IV discusses the optimization of beam divergence, magnification, and timing; Sec. V discusses the design of radiochromic (RC) film packs for proton measurements; Sec. VI presents the first results of this method; Sec. VII gives some characteristics of common failures for troubleshooting TNSA backlighting; and finally the paper is concluded in Sec. VIII.

II. EXPERIMENTAL OVERVIEW

The OMEGA facility[2] is a 60-beam frequency-tripled Nd:glass laser that produces up to 30 kJ UV in 1 ns to several ns long pulses. The OMEGA EP petawatt laser facility[3] has two "long-pulse" beams (order ns), and two "short-pulse" beams (1–100 ps pulses). One of the short pulse beams can be transported to the OMEGA target chamber for joint shot operations. Currently, the system is capable of ~300 J UV in 1 ps or ~1 kJ UV in 10 ps.[59]

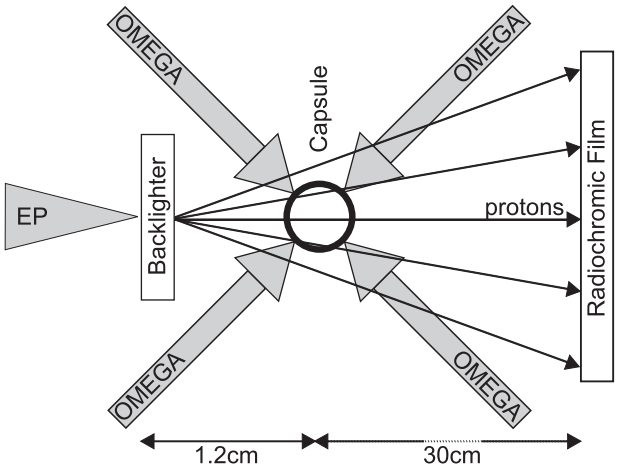

FIG. 1. Top-level schematic of the experiment. Sixty OMEGA beams drive a spherical implosion, which is backlight by the EP laser-generated protons and imaged on a radiochromic film detector.

In this experiment, all 60 OMEGA beams drive the subject spherical capsule implosion. A top-level schematic of the experiment is shown in Fig. 1. The target is a 20–40 μm thick plastic (CH) shell of outer diameter 860 μm filled with ^{4}He gas at 18 atm. The OMEGA pulse shape is a 3.5 ns 17 kJ "shock ignition" pulse[5] using smoothing by spectral dispersion[60] and SG4 phase plates,[61] as the ultimate physics goal is to study the shock propagation in the imploded capsule.[6] The capsule drive pulse is started several ns before the backlighter is fired, as the most interesting physics occurs when the shock is launched, as well as near peak neutron production and stagnation. The backlighter foil used was 10 μm thick Au. A 1 ps 300 J OMEGA EP short-pulse beam was used for TNSA backlighting, with a focal spot size ~40μm in diameter for an intensity $\approx 2 \times 10^{19}$ W/cm^2.

III. BACKLIGHTER DESIGN

As listed in the Introduction, there are three main mechanisms that could degrade the backlighter performance in this environment.

A. Preplasma

It is known that any prepulse on the proton-generating laser beam can create a "preplasma" at the target that dramatically reduces the backlighter performance.[29] In this experiment, the subject capsule is imploded via 60-OMEGA beams via ablation pressure. The ablated mass is ejected outward to large radii, forming a large coronal plasma around the implosion. Since the capsule drive starts several ns before backlighting, the coronal plasma can reach the backlighter. In a simple geometry, shown in Fig. 2, the coronal plasma flows around the backlighter foil and can impede the short-pulse beam propagation to the solid foil surface. This has the same effect as preplasma: the conversion efficiency from laser energy to energetic protons is greatly reduced. Additionally, coronal plasma at the backlighter target can short out the sheath field due to Debye screening; this will also reduce the

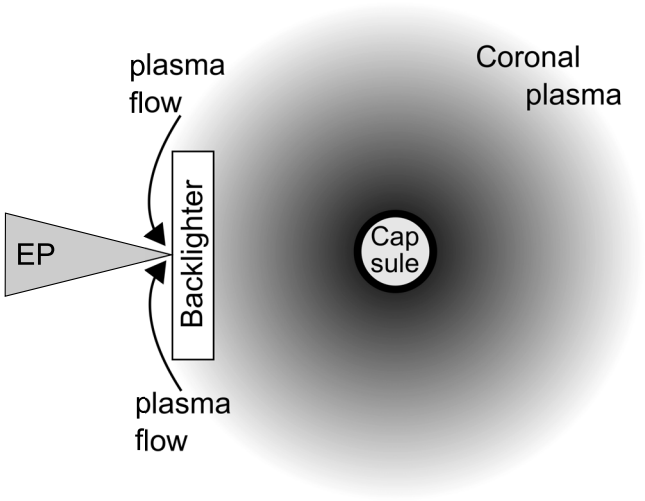

FIG. 2. A coronal plasma forms around an imploding capsule due to ablation blow off from the OMEGA drive. The coronal plasma can flow around the backlighter foil to reach where the short-pulse beam propagates. This impedes the short-pulse propagation to the focal point, leading to reduced proton maximum energy and yield.

conversion efficiency. The backlighter shielding must therefore be designed to impede the coronal plasma flow so that it does not interact with the target.

B. X-ray cross talk

X-ray imaging of capsule implosions shows that the capsule emits x rays during the drive.[62] These x rays are emitted isotropically, so some fraction will be incident on the backlighter foil. This is shown schematically in Fig. 3. The x rays will efficiently heat the Au backlighter foil, which can create some preplasma on the back surface approximately ns before the short-pulse beam is incident on the foil. This would be a similar effect to a prepulse on the short-pulse beam, or interference by coronal plasma. To mitigate this effect the backlighter foil must be shielded from "cross talk" from the capsule.

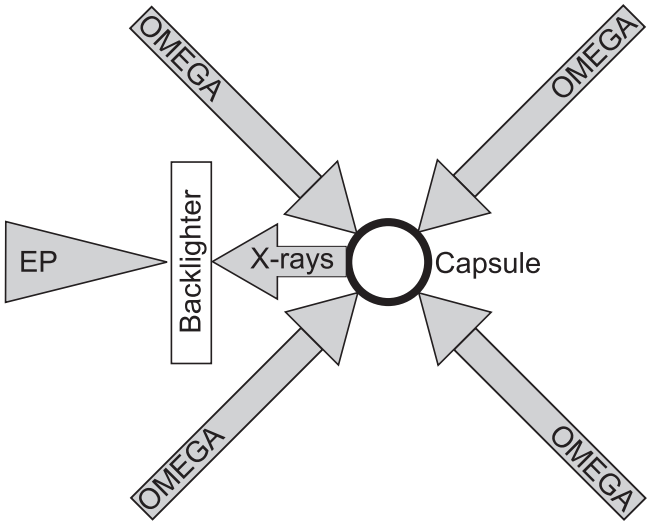

FIG. 3. Sixty OMEGA beams drive the capsule implosion. X rays from the capsule can preheat the backlighter foil, which will reduce the backlighter performance.

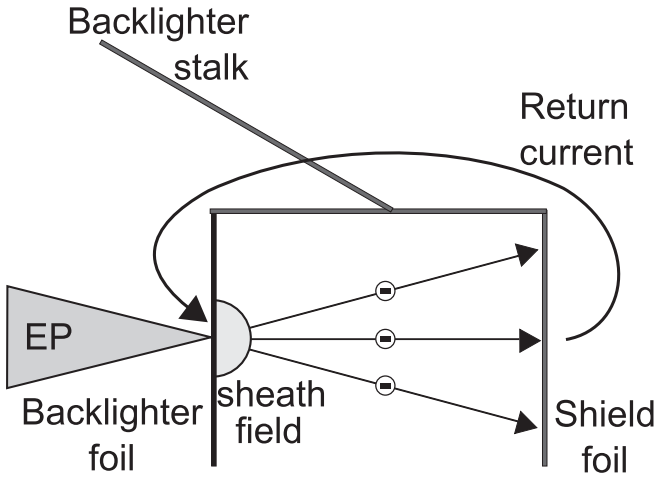

FIG. 4. If there is a pathway for fast electrons to form a return current to the backlighter foil within the backlighter pulse, then the sheath field can be neutralized. This reduces TNSA production. Return current can be mitigated by ensuring that the target scale lengths are large enough that the current cannot flow during the pulse duration.

C. Return current

In the TNSA mechanism, fast electrons escape from the backlighter foil due to the high-intensity laser-matter interaction. This sets up a strong electric sheath field, which accelerates the protons of interest for TNSA backlighting. If, for example, a shield foil is placed in front (toward the implosions) of the backlighter foil to shield from x-ray cross talk (Sec III B), as shown in Fig. 4, then there is a potential for the fast electrons to generate a return current loop back to the backlighter foil. This would neutralize the acceleration sheath field, and reduce the backlighter proton performance.

Therefore, the backlighter size must be greater than the scale length $\ell = c\tau$, where τ is the laser pulse length, and the electrons are ultra-relativistic ($v \approx c$). With a 1 ps pulse $\ell \sim 0.3$ mm, and at $\tau = 10$ ps the scale length $\ell \sim 3$ mm. Since typical backlighter sizes are of order mm, this is a design concern for 10 ps pulses but not 1 ps ones.

D. Resulting design

A backlighter for joint OMEGA and EP TNSA radiography has been designed to mitigate these issues. A schematic is shown in Fig. 5, and fabricated backlighters are shown in Fig. 6.

The 10 μm Au foil is the actual backlighter foil target. The foil is glued to a 1 mm thick CH washer. On the other end of the washer, a 3 μm Ta foil acts as a x-ray cross talk shield. The washer is encased in a thin brass cylindrical shell that forms a shield to impede coronal plasma flow to the backlighter foil. As shown in Fig. 5 the EP beam comes in from the left, and TCC is to the right. As a 1 ps pulse is used in these experiments, there is no potential for return current issues due to the scale lengths of this backlighter design.

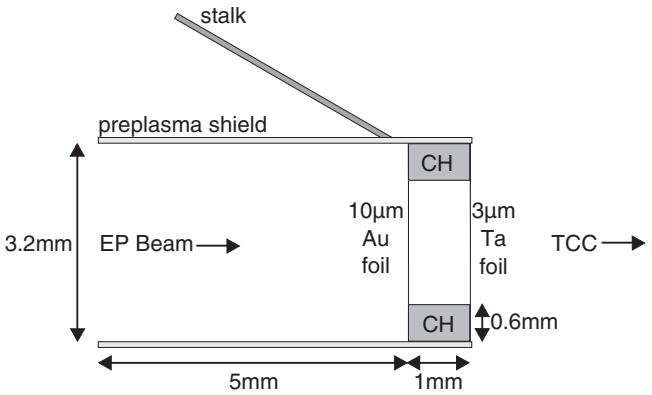

FIG. 5. Backlighter design used in these experiments. Shown is a cross section, where the design has cylindrical symmetry around the central axis (except for the target-positioned stalk).

IV. EXPERIMENTAL OPTIMIZATION

The experimental configuration, i.e., separation between backlighter, subject, and imaging plane, must be adjusted to optimize the backlighter performance, magnification, and radiography timing. The backlighter-capsule distance d_o and the capsule-film distance d_i are shown in Fig. 7.

The TNSA-generated proton beam has a cone-shaped emission, so with a given beam intensity a larger d_i results in less fluence on the detector. In joint radiography experiments we observed that the film pack performs well for $d_i \sim 30$ cm.

The magnification is

$$M = \frac{d_i + d_o}{d_o} = 1 + \frac{d_i}{d_o}. \quad (1)$$

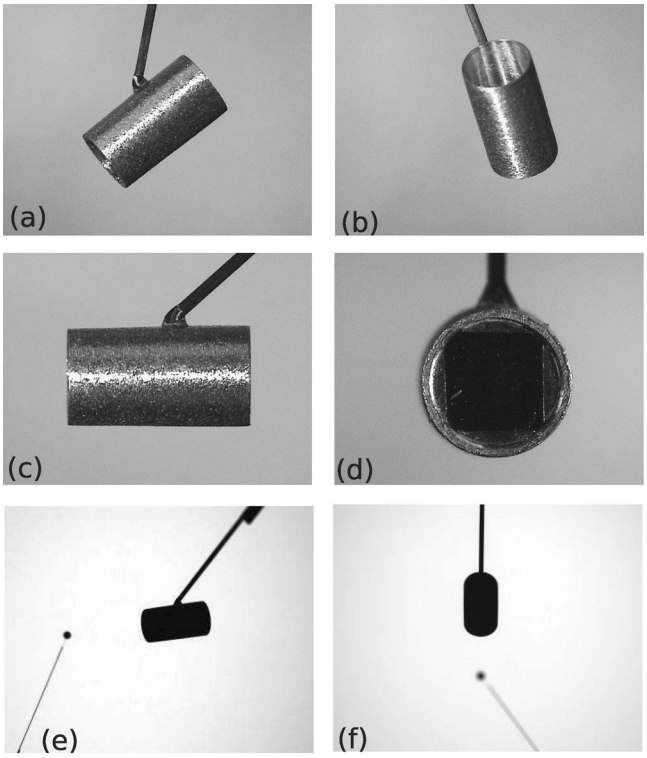

FIG. 6. Images of fielded backlighters. From top to left: (a) and (b) two isometric views of a backlighter, (c) side-on view of backlighter, (d) view from TCC of backlighter, and (e) and (f) shadowgraphs of pre-shot backlighter and capsule in OMEGA target chamber.

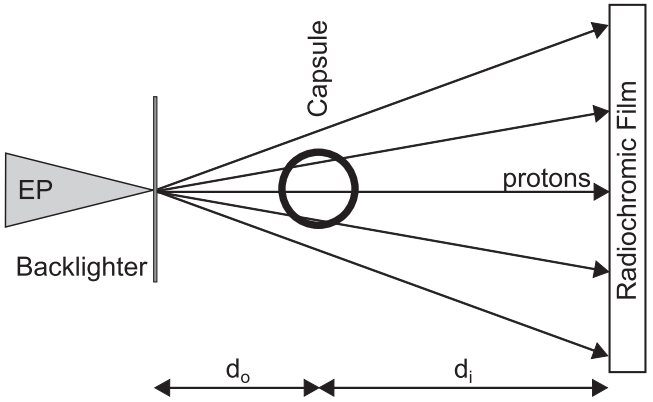

FIG. 7. The radiography time-of-flight, magnification, and EP backlighter performance depend on the backlighter-object distance (d_o) and object-film distance (d_i). Optimized values, as used in these experiments, are $d_o = 1.2$ cm and $d_i \sim 30$ cm.

Since the interesting physics in a capsule implosions happens at small radii, $\leq$200 μm, the magnification must be at least 25 for detectable features. With $d_i \approx 30$ cm, this constrains $d_o \leq 1.25$ cm. Depending on the experimental goals a higher magnification may be desirable.

The radiography time-of-flight (TOF) depends on the choice of d_o. Since the TNSA mechanism produces a falling exponential distribution with proton energy,[25] low- (several MeV) and high- (several tens of MeV) energy protons can be used to backlight the implosion at differing times of flight.[9,51] All protons are born essentially simultaneously, within 1–10 ps depending on the high-intensity laser pulse length, so each proton energy backlights the implosion at a time,

$$t = \tau + d_o/v_p, \quad (2)$$

where τ is the short-pulse laser delay, and $v_p = v_p(E)$ is the proton velocity. The time window radiographed in one shot is

$$\delta t = d_o \left(\frac{1}{v_{p,min}} - \frac{1}{v_{p,max}} \right), \quad (3)$$

where $v_{p,\,min}$ and $v_{p,\,max}$ are, respectively, the minimum and maximum energies for which usable radiographs are obtained. Ideally this is $\geq$150 ps to allow radiography of a large total time window of the implosion physics. This is easily achievable with the film pack design in this paper for $d_o = 1.2$ cm, as will be shown in Sec. V.

V. FILM PACK DESIGN

The film pack used in these experiments is shown in Fig. 8. Protons from the backlighter are incident from the

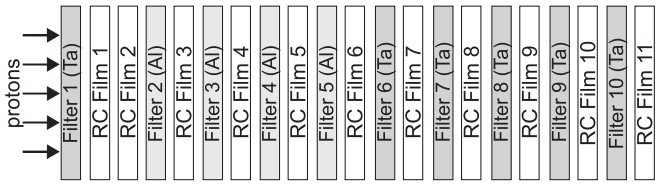

FIG. 8. Radiochromic (RC) film pack design for detection of proton radiographs. The pack consists of interleaved filters (Al or Ta) and films.

TABLE I. Film pack filter materials and thicknesses.

Filter	Material	Thickness (μm)
1	Ta	42
2	Al	29
3	Al	106
4	Al	205
5	Al	480
6	Ta	390
7	Ta	407
8	Ta	534
9	Ta	1027
10	Ta	1026

left. A series of Al or Ta filters and Gafchromic® HD-810 radiochromic films[63] are interleaved. The filter pack transverse size is 10cm × 10cm. Each filter is measured with a micrometer since the thickness tolerance is generally 10% (standard filter stock from Goodfellow® (Ref. 64)). Each filter's material and measured thickness is listed in Table I.

With known filter thicknesses and composition information on the HD-810 film, the proton energy that each film is primarily sensitive to, ϵ, is calculated using SRIM (Ref. 65) calculated stopping powers. This is done by calculating the deposited energy per incident proton energy for initial proton energies from 0 to 60 MeV. This is shown for a specific RC film 5 in Fig. 9.

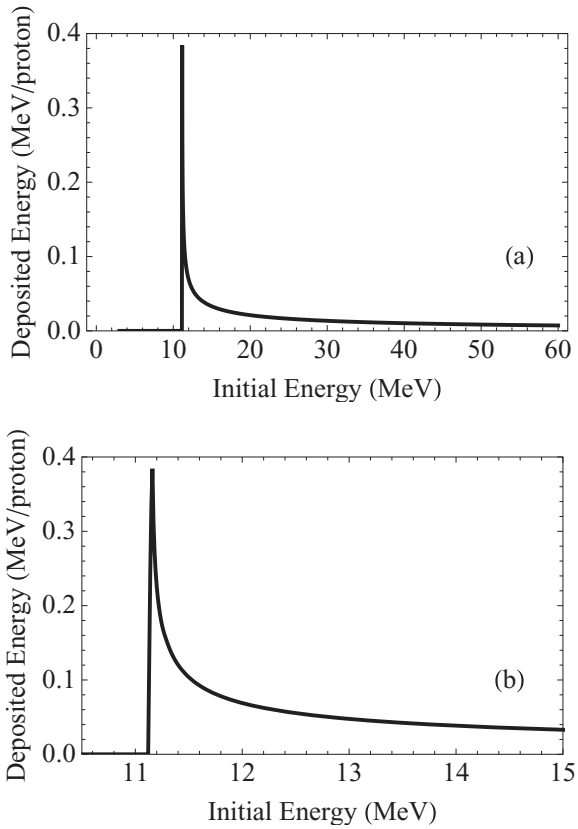

FIG. 9. Sensitivity versus proton energy for film 5, chosen as an example of typical behavior. (a) Full range of proton energies typically produced. (b) Zoomed in view of the peak structure.

TABLE II. Film pack proton energy of maximum sensitivity, ϵ, and time-of-flight (TOF) to the subject implosion d_o/v_p for $d_o = 1.2$ cm.

Film	ϵ (MeV)	TOF (ns)
1	3.8	0.64
2	5.2	0.54
3	6.6	0.48
4	8.6	0.42
5	11.2	0.37
6	15.3	0.32
7	22.8	0.26
8	29.4	0.23
9	36.8	0.21
10	48.4	0.18
11	58.4	0.17

ϵ is used to calculate a time-of-flight for each film, corresponding to when that radiograph is taken. This information is given in Table II.

In future experiments, the magnification will be increased by decreasing d_o. In this case it is useful to show how the sample timing changes with d_o. The TOF curve for arbitrary proton energy, with chosen film energies marked, is shown in Fig. 10 for $d_o = 0.6$, 0.9, 1.2 cm.

Another film pack consideration is the high-energy tail to the film sensitivity, as can be seen in Fig. 9. The peak sensitivity (Fig. 9) is narrow due to the Bragg peak, but the integrated tail as shown for a single film sensitivity is significant. The TNSA proton mechanism produces a falling exponential energy distribution that suppresses the high-energy tail of the sensitivity. The approximate distribution is folded with the sensitivities calculated for each film, as shown in Figs. 11 and 12. In future shots the last 2–3 films will be replaced by higher sensitivity Gafchromic® MD-V2-55 films.

In future experiments the proton distribution can be measured by taking a backlighter-only shot. With a microdensitometer or optical microscope to measure the film optical density and known film response, the exact proton fluence can be calculated using this sensitivity method.[66]

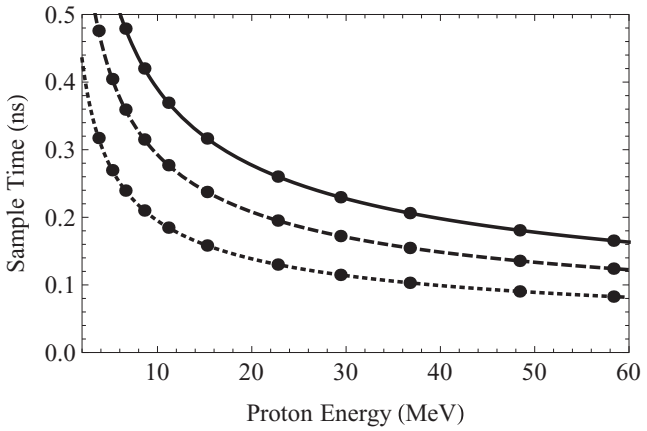

FIG. 10. Time-of-flight curves for $d_o = 0.6$ cm (dotted line), = 0.9 cm (dashed line), and = 1.2 cm (solid line). The points mark specific film energies (see Table II).

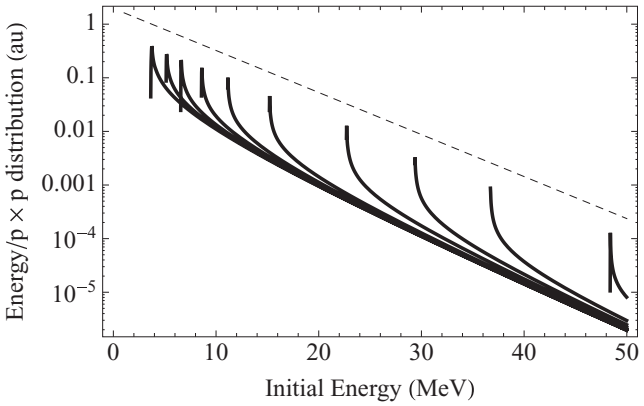

FIG. 11. RC film sensitivity, as energy deposited per proton, folded with an assumed exponential proton distribution and plotted versus initial energy. Ten of 11 films are shown, from film 1 to 10 from left to right (Film 11 is of-scale to the right). The dashed line represents the assumed exponential normalized source distribution.[25]

VI. RESULTS

Using the techniques outlined in Secs. III–V, a series of radiographs was taken of the filamentary electromagnetic field structure around an imploded capsule. Four sequential films are shown in Fig. 13. This data was taken with the film pack configured as in Sec. V, with a 17 kJ shock ignition pulse (FIS3601P) (Ref. 5) driving the capsule with all 60 OMEGA beams, and a 300 J 1 ps EP pulse generating the backlighting protons, using the backlighter design in Sec. III. For this shot $d_o = 1.2$cm and $d_i = 30$ cm, so the magnification is 26 and the RC film field of view is 3.8mm at the target plane. Timing of the short-pulse beam relative to the implosion drive, and subsequent proton sampling times, is shown in Fig. 13(e).

The filamentary structures that dominate the radiographs in Fig. 13 are the result of proton deflections resulting from the Lorentz force. Large self-generated fields have been previously observed in the corona of directly driven ICF implosions, and the physics of these fields has been studied by Séguin *et al.*[67] Previous TNSA-backlit implosions[9] did not show such filamentary structures, but other experiments have.[10] This was due to much lower laser intensity on the implosion target in these previous TNSA experiments, and demonstrates the importance of this backlighting capability for full-energy implosions. These filamentary structures are not seen in indirect-drive implosions.[15]

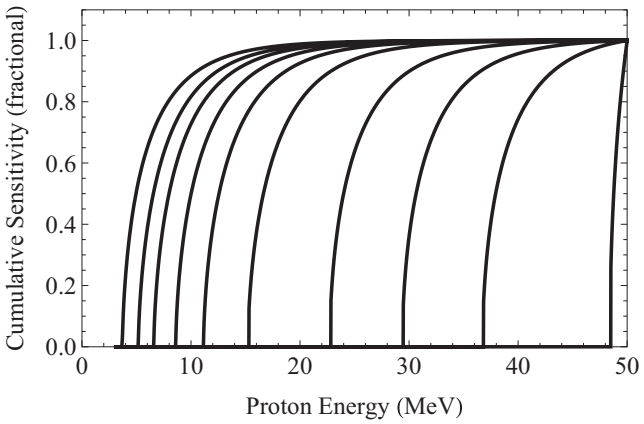

FIG. 12. RC film sensitivity, as cumulative energy deposited for protons with energy $\leq E$ vs E (i.e., a running integral of Fig. 11. Each film is normalized to the total sensitivity. Ten of 11 films are shown, from film 1 to 10 from left to right (Film 11 is off scale to the right).

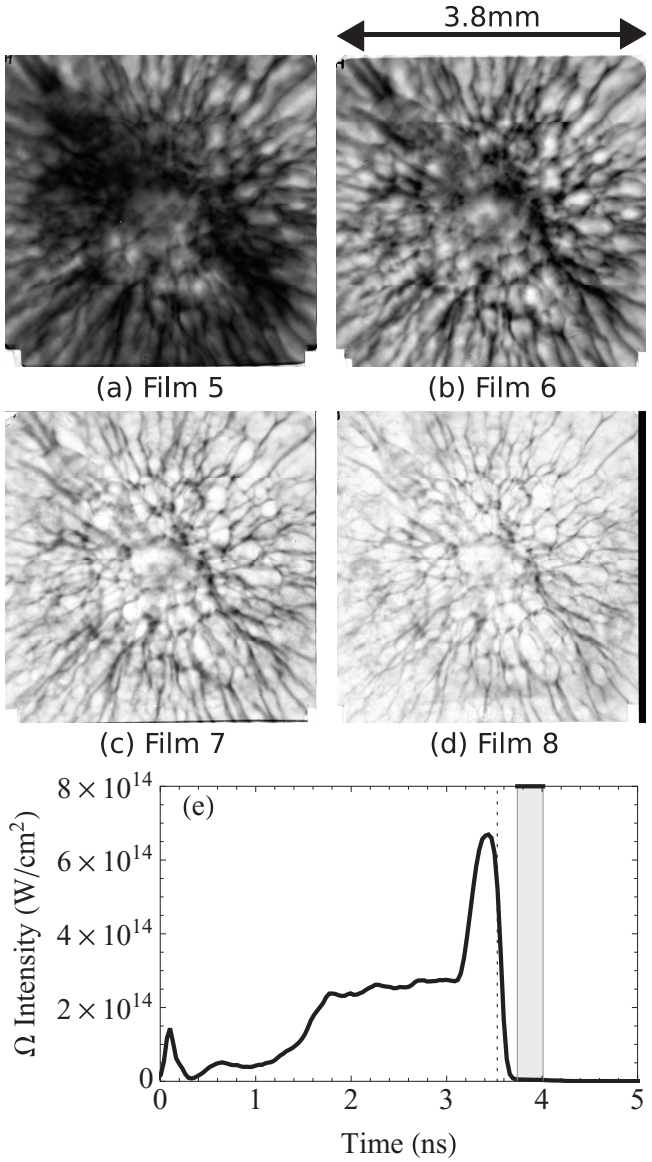

FIG. 13. (a)–(d) A series of radiographs of the filamentary field structure around an imploded capsule, OMEGA shot 61 250. For film energies and timing, see Table II. (e) Timing for OMEGA shot 61 250, corresponding to radiography presented in (a)–(d). The black curve represents the average OMEGA implosion drive intensity (pulse shape FIS3601P) as measured on shot. The vertical dashed line shows when the EP short pulse beam was fired. The gray box represents the sample times for Films 3 through 9, which recorded useful data on this implosion (see also Table II).

Additionally, the protons are sensitive to the line integrated areal density between the backlighter and film through the charged-particle stopping power,

$$\Delta E = \int \frac{dE}{d\rho R} \mathrm{d}\rho \mathrm{R}, \tag{4}$$

which will be used in future experiments.

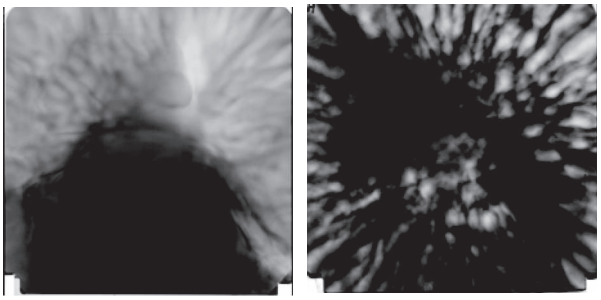

FIG. 14. Comparison of 60-beam OMEGA radiographs using backlighters without (left) and with (right) a preplasma shield, as discussed in Sec. III. The implosion is at the center of each image; (a) is dominated by large-scale diffuse structure and (b) is dominated by filamentary field structures.

VII. DIAGNOSING FAILED RADIOGRAPHY

If a radiography shot fails, it is important to troubleshoot the failure with the smallest number of additional shots and least amount of time, given the experimental constraints at facilities such as OMEGA and OMEGA EP. On a typical joint shot day, a principal investigator (PI) can expect 6 ± 1 radiography shots. Two common failures were observed backlighting implosions.

The preplasma issue, as discussed in Sec. III A and Fig. 2, can seriously degrade the backlighter performance. When the coronal plasma interferes with the EP beam propagation, the proton beam emission is more diffuse and the highest energy proton produced is low (10–20 MeV instead of ~50). Diffuse large-scale structures have been observed in this case, as shown in Fig. 14. The left image shows a radiograph where the backlighter did not have a preplasma shield, and the right image had a shield as detailed in Sec. III. On the left some filamentary structure is observed in the top left and top right, but most of the image is dominated by a large diffuse structure resulting from the coronal plasma interaction with the backlighter. On the right, with a shield, a radiograph of the entire implosion is obtained, demonstrating the backlighter performance improvement with the shield.

If the film pack is too far away (d_i is too large) then the TNSA proton beam divergence can mean that the fluence on the detector is too low. If this is the case, then it affects the high-energy films first due to the exponential distribution. Thus, a low proton energy cut-off (10–20 MeV instead of ~50) but sharp radiographs at low energy results from d_i being too large. This is shown in Fig. 15, a radiograph of an unimploded capsule with the lowest energy film at $d_i = 69$ cm. The higher energy films did not have visible radiographs. With an optimal $d_i = 30$ cm the higher fluence saturates the lowest energy film but at higher energies excellent radiographs are obtained (shown in Fig. 13).

VIII. CONCLUSIONS AND FUTURE WORK

Petawatt-class lasers with kilojoule-picosecond pulses offer new opportunities for ICF and high-energy density physics (HEDP) radiography, including using the TNSA energetic proton production mechanism for proton backlighting. This technique offers better spatial and temporal resolution but poorer spatial uniformity and energy resolution than previous fusion-based proton backlighters. It offers a wide range of proton energies which is beneficial for mapping out field structures in ICF and HEDP plasmas. We present the first results of using TNSA proton backlighting to image 60-beam OMEGA implosions. In such experiments there are several challenges using the TNSA mechanism to generate backlighting protons, such as avoiding preplasma, cross talk, return current, and optimizing the experimental configuration to achieve the desired magnification, timing, and fluence at the radiochromic film detector. This work presents solutions to this issues that will allow future joint OMEGA and OMEGA EP experiments to use TNSA backlighting to study ICF and HEDP physics. In contrast to previous TNSA implosion radiography,[9] we observe strong filamentary EM field structures[67] around the implosion that result from higher implosion drive intensity and illustrate the need for the capability to backlight full-energy implosions.

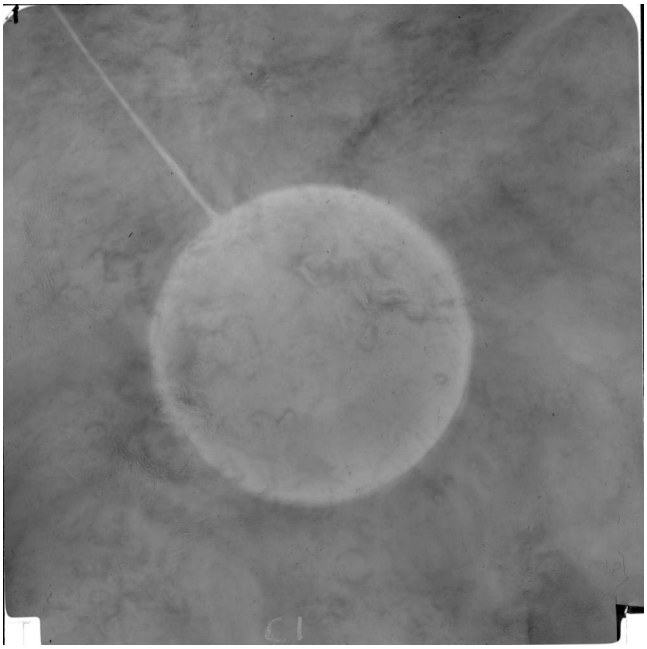

FIG. 15. Film 1, $d_i = 69$cm, OMEGA shot 61 247. The image is of an undriven implosion. In this case, d_i is too large so only the lowest proton energy film recorded useful data. On a nominal performance backlighter shot, with d_i optimized, Film 1 saturates.

This technique will be applied to study shock propagation in shock ignition implosions at OMEGA, in particular, using high-energy protons to probe the electromagnetic field structure at the shock front. The improved spatial and temporal resolution will be used to study electromagnetic fields in hohlraums around the laser entrance hole and at plasma bubbles formed at the wall, expanding on previous efforts.[14–16]

The future NIF Advanced Radiographic Capability (ARC) (Ref. 68) will allow the study of full-scale NIF experiments using a petawatt-class laser. Radiography using NIF ARC will be at similar backlighter drive conditions to OMEGA EP (kilojoule-picosecond pulses), and with additional but similar challenges to those discussed in this work due to 60 times more subject drive energy at NIF. NIF ARC proton radiography will provide an important diagnostic for

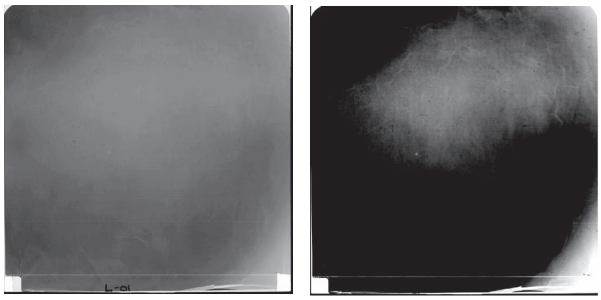

FIG. 16. Film 1, OMEGA shot 63 031. (a) Normal film scan and (b) enhanced contrast image. The EP backlighter was fired at reduced energy (40 J) for timing purposes without an implosion target in place, which also gives a uniformity measure. Here we can see some low-amplitude large-scale spatial non-uniformities, but clearly distinct from implosion effects in Fig. 13.

electromagnetic field structures in megajoule indirect- and direct-drive implosions. It will be important to transfer experience with TNSA backlighting from full-scale joint OMEGA experiments, as discussed in this work, to future radiography using ARC on the NIF.

ACKNOWLEDGMENTS

This work was done in partial fulfillment of the requirements for the degree of Ph.D. (A.B.Z.). The authors thank the engineering and operations staff at the OMEGA and OMEGA EP facilities for their support. This work was supported in part by (U.S.) Department of Energy (DOE) and LLE National Laser User's Facility (DE-FG52-07NA28059 and DE-FG03-03SF22691), LLNL (B543881 and LDRD-ER-898988), LLE (414090-G), FSC at the University of Rochester (412761-G), and General Atomics (DE- AC52-06NA 27279). A. Zylstra is supported by the DOE NNSA Stewardship Science Graduate Fellowship (DE-FC52-08NA28752).

APPENDIX: BACKLIGHTER UNIFORMITY

Recent data taken demonstrates the general uniformity of the TNSA backlighter. This data is shown in Fig. 16. The image is from a 40 J 1 ps short-pulse shot onto a normal backlighter target, but without an implosion target in place. The primary purpose of the shot is facility timing. We can see low-amplitude large-scale spatial variations of the order of the image size, but no higher order source non-uniformities that could be confused with physics effects seen in the implosion (Fig. 13).

In future experiments this could be investigated for a full-energy backlighter drive, which was not done in present experiments due to a limited number of shots. Additionally, in experiments where precise spectral information is required, a source proton spectrum could be measured on a similar full-energy null shot. This would be particularly important for measuring areal densities of imploded shells with proton backlighters.

[1]G. Miller, E. Moses, and C. Wuest, Nucl. Fusion **44**, S228 (2004).
[2]T. Boehly, D. Brown, R. Craxton, R. Keck, J. Knauer, J. Kelly, T. Kessler, S. Kumpan, S. Loucks, S. Letzring, F. Marshall, R. McCrory, S. Morse, W. Seka, J. Soures, and C. Verdon, Opt. Commun. **133**, 495 (1997).
[3]L. Waxer, D. Maywar, J. Kelly, T. Kessler, B. Kruschwitz, S. Loucks, R. McCrory, D. Meyerhofer, S. Morse, C. Stoeckl, and J. Zuegel, Opt. Photonics News **16**, 30 (2005).
[4]R. S. Craxton, F. J. Marshall, M. J. Bonino, R. Epstein, P. W. McKenty, S. Skupsky, J. A. Delettrez, I. V. Igumenshchev, D. W. Jacobs-Perkins, J. P. Knauer, J. A. Marozas, P. B. Radha, and W. Seka, Phys. Plasmas **12**, 056304 (2005).
[5]R. Betti, C. Zhou, K. Anderson, L. Perkins, W. Theobald, and A. Solodov, Phys. Rev. Lett. **98**, 155001 (2007).
[6]D. D. Meyerhofer, R. L. McCrory, R. Betti, T. R. Boehly, D. T. Casey, T. J. B. Collins, R. S. Craxton, J. A. Delettrez, D. H. Edgell, R. Epstein, K. A. Fletcher, J. A. Frenje, Y. Yu. Glebov, V. N. Goncharov, D. R. Harding, S. X. Hu, I. V. Igumenshchev, J. P. Knauer, C. K. Li, J. A. Marozas, F. J. Marshall, P. W. McKenty, P. M. Nilson, S. P. Padalino, R. D. Petrasso, P. B. Radha, S. P. Regan, T. C. Sangster, F. H. Seguin, W. Seka, R. W. Short, D. Shvarts, S. Skupsky, J. M. Soures, C. Stoeckl, W. Theobald, and B. Yaakobi, Nucl. Fusion **51**, 053010 (2011).
[7]R. Tommasini, A. MacPhee, D. Hey, T. Ma, C. Chen, N. Izumi, W. Unites, A. MacKinnon, S. Hatchett, B. Remington, H. Park, P. Springer, J. Koch, O. Landen, J. Seely, G. Holland, and L. Hudson, Rev. Sci. Instrum. **79**, 10E901 (2008).
[8]F. Marshall, P. McKenty, J. Delettrez, R. Epstein, J. Knauer, V. Smalyuk, J. Frenje, C. Li, R. Petrasso, F. Séguin, and R. Mancini, Phys. Rev. Lett. **102**, 185004 (2009).
[9]A. J. Mackinnon, P. K. Patel, M. Borghesi, R. C. Clarke, R. R. Freeman, H. Habara, S. P. Hatchett, D. Hey, D. G. Hicks, S. Kar, M. H. Key, J. A. King, K. Lancaster, D. Neely, A. Nikkro, P. A. Norreys, M. M. Notley, T. W. Phillips, L. Romagnani, R. A. Snavely, R. B. Stephens, and R. P.J. Town, Phys. Rev. Lett. **97**, 045001 (2006).
[10]J. Rygg, F. Séguin, C. Li, J. Frenje, M. Manuel, R. Petrasso, R. Betti, J. Delettrez, O. Gotchev, J. Knauer, D. Meyerhofer, F. Marshall, C. Stoeckl, and W. Theobald, Science **319**, 1223 (2008).
[11]C. Li, F. Seguin, J. Frenje, J. Rygg, R. Petrasso, R. Town, P. Amendt, S. Hatchett, O. Landen, A. Mackinnon, P. Patel, V. Smalyuk, J. Knauer, T. Sangster, and C. Stoeckl, Rev. Sci. Instrum. **77**, 10E725 (2006).
[12]C. Li, F. Séguin, J. Rygg, J. Frenje, M. Manuel, R. Petrasso, R. Betti, J. Delettrez, J. Knauer, F. Marshall, D. Meyerhofer, D. Shvarts, V. Smalyuk, C. Stoeckl, O. Landen, R. Town, C. Back, and J. Kilkenny, Phys. Rev. Lett. **100**, 225001 (2008).
[13]C. Li, F. Séguin, J. Frenje, M. Manuel, R. Petrasso, V. Smalyuk, R. Betti, J. Delettrez, J. Knauer, F. Marshall, D. Meyerhofer, D. Shvarts, C. Stoeckl, W. Theobald, J. Rygg, O. Landen, R. Town, P. Amendt, C. Back, and J. Kilkenny, Plasma Phys. Control. Fusion **51**, 014003 (2009).
[14]C. Li, F. Séguin, J. Frenje, R. Petrasso, P. Amendt, R. Town, O. Landen, J. Rygg, R. Betti, J. Knauer, D. Meyerhofer, J. Soures, C. Back, J. Kilkenny, and A. Nikroo, Phys. Rev. Lett. **102**, 205001 (2009).
[15]C. Li, F. Séguin, J. Frenje, M. Rosenberg, R. Petrasso, P. Amendt, J. Koch, O. Landen, H. Park, H. Robey, R. Town, A. Casner, F. Philippe, R. Betti, J. Knauer, D. Meyerhofer, C. Back, J. Kilkenny, and A. Nikroo, Science **327**, 1231 (2010).
[16]C. Li, F. Séguin, J. Frenje, M. Rosenberg, A. Zylstra, R. Petrasso, P. Amendt, J. Koch, O. Landen, H. Park, H. Robey, R. Town, A. Casner, F. Philippe, R. Betti, J. Knauer, D. Meyerhofer, C. Back, J. Kilkenny, and A. Nikroo, Plasma Phys. Control. Fusion **52**, 124027 (2010).
[17]C. Li, F. Séguin, J. Frenje, J. Rygg, R. Petrasso, R. Town, P. Amendt, S. Hatchett, O. Landen, A. Mackinnon, P. Patel, V. Smalyuk, T. Sangster, and J. Knauer, Phys. Rev. Lett. **97**, 135003 (2006).
[18]C. Li, F. Séguin, J. Frenje, J. Rygg, R. Petrasso, R. Town, P. Amendt, S. Hatchett, O. Landen, A. Mackinnon, P. Patel, M. Tabak, J. Knauer, T. Sangster, and V. Smalyuk, Phys. Rev. Lett. **99**, 15001 (2007).
[19]C. Li, F. Séguin, J. Frenje, J. Rygg, R. Petrasso, R. Town, O. Landen, J. Knauer, and V. Smalyuk, Phys. Rev. Lett. **99**, 55001 (2007).
[20]R. Petrasso, C. Li, F. Seguin, J. Rygg, J. Frenje, R. Betti, J. Knauer, D. Meyerhofer, P. Amendt, D. Froula, O. Landen, P. Patel, J. Ross, and R. Town, Phys. Rev. Lett. **103**, 85001 (2009).
[21]C. Li, F. Séguin, J. Frenje, M. Manuel, D. Casey, N. Sinenian, R. Petrasso, P. Amendt, O. Landen, J. Rygg, R. Town, R. Betti, J. Delettrez, J. Knauer, F. Marshall, D. Meyerhofer, T. Sangster, D. Shvarts, V. Smalyuk, J. Soures, C. Back, J. Kilkenny, and A. Nikroo, Phys. Plasmas **16**, 056304 (2009).
[22]J. Badziak, Opto-Electron. Rev. **15**, 1 (2007).
[23]P. Norreys, Nature Photonics **3**, 423 (2009).
[24]S. Hatchett, C. Brown, T. Cowan, E. Henry, J. Johnson, M. Key, J. Koch, A. Langdon, B. Lasinski, R. Lee, A. Mackinnon, D. Pennington, M. Perry,

T. Phillips, M. Roth, T. Sangster, M. Singh, R. Snavely, M. Stoyer, S. Wilks, and K. Yasuike, Phys. Plasmas **7**, 2076 (2000).
[25]R. Snavely, M. Key, S. Hatchett, T. Cowan, M. Roth, T. Phillips, M. Stoyer, E. Henry, T. Sangster, M. Singh, S. Wilks, A. MacKinnon, A. Offenberger, D. Pennington, K. Yasuike, A. Langdon, B. Lasinski, J. Johnson, M. Perry, and E. Campbell, Phys. Rev. Lett. **85**, 2945 (2000).
[26]A. Fews, P. Norreys, F. Beg, A. Bell, A. Dangor, C. Danson, P. Lee, and S. Rose, Phys. Rev. Lett. **73**, 1801 (1994).
[27]K. Krushelnick, E. Clark, M. Zepf, J. Davies, F. Beg, A. Machacek, M.
Santala, M. Tatarakis, I. Watts, P. Norreys, and A. Dangor, Phys. Plasmas **7**, 2055 (2000).
[28]A. Maksimchuk, S. Gu, K. Flippo, D. Umstadter, and V. Bychenkov, Phys. Rev. Lett. **84**, 4108 (2000).
[29]A. Mackinnon, M. Borghesi, S. Hatchett, M. Key, P. Patel, H. Campbell, A. Schiavi, R. Snavely, S. Wilks, and O. Willi, Phys. Rev. Lett. **86**, 1769 (2001).
[30]A. Mackinnon, Y. Sentoku, P. Patel, D. Price, S. Hatchett, M. Key, C. Andersen, R. Snavely, and R. Freeman, Phys. Rev. Lett. **88**, 215006 (2002).
[31]M. Roth, A. Blazevic, M. Geissel, T. Schlegel, T. Cowan, M. Allen, J. Gauthier, P. Audebert, J. Fuchs, J. Meyer-ter Vehn, M. Hegelich, S. Karsch, and A. Pukhov, Phys. Rev. ST Accel. Beams **5**, 61301 (2002).
[32]M. Roth, M. Allen, P. Audebert, A. Blazevic, E. Brambrink, T. Cowan, J. Fuchs, J. Gauthier, M. Geißel, M. Hegelich, S. Karsch, J. Meyer-ter Vehn, T. Ruhl, H aand Schlegel, and R. Stephens, Plasma Phys. Control. Fusion **44**, B99 (2002).
[33]M. Zepf, E. Clark, F. Beg, R. Clarke, A. Dangor, A. Gopal, K. Krushelnick, P. Norreys, M. Tatarakis, U. Wagner, and M. Wei, Phys. Rev. Lett. **90**, 64801 (2003).
[34]M. Allen, P. Patel, A. Mackinnon, D. Price, S. Wilks, and E. Morse, Phys. Rev. Lett. **93**, 265004 (2004).
[35]M. Borghesi, A. J. Mackinnon, D. H. Campbell, D. G. Hicks, S. Kar, P. K. Patel, D. Price, L. Romagnani, A. Schiavi, and O. Willi, Phys. Rev. Lett. **92**, 055003 (2004).
[36]J. Fuchs, P. Antici, E. D'Humieres, E. Lefebvre, M. Borghesi, E.
Brambrink, C. Cecchetti, M. Kaluza, V. Malka, M. Manclossi, S. Meyroneinc, P. Mora, J. Schreiber, T. Toncian, H. Pepin, and P. Audebert, Nat. Phys. **2**, 48 (2005).
[37]J. Fuchs, Y. Sentoku, S. Karsch, J. Cobble, P. Audebert, A. Kemp, A. Nikroo, P. Antici, E. Brambrink, A. Blazevic, E. Campbell, J. Fernandez, J. Gauthier, M. Geissel, M. Hegelich, H. Pepin, H. Popescu, N. Renard-LeGalloudec, M. Roth, J. Schreiber, R. Stephens, and T. Cowan, Phys. Rev. Lett. **94**, 45004 (2005).
[38]L. Romagnani, J. Fuchs, M. Borghesi, P. Antici, P. Audebert, F. Ceccherini, T. Cowan, T. Grismayer, S. Kar, A. Macchi, P. Mora, G. Pretzler, A. Schiavi, T. Toncian, and O. Willi, Phys. Rev. Lett. **95**, 195001 (2005).
[39]M. Borghesi, J. Fuchs, S. Bulanov, A. Mackinnon, P. Patel, and M. Roth, Fusion Sci. Technol. **49**, 412 (2006).
[40]D. Neely, P. Foster, A. Robinson, F. Lindau, O. Lundh, A. Persson, C. Wahlstr"om, and P. McKenna, Appl. Phys. Lett. **89**, 021502 (2006).
[41]K. Flippo, T. Bartal, F. Beg, S. Chawla, J. Cobble, S. Gaillard, D. Hey, A. MacKinnon, A. MacPhee, P. Nilson, D. Offermann, S. Le Pape, and M. Schmitt, J. Phys: Conf. Ser. **244**, 022033 (2010).
[42]K. Flippo, T. Bartal, F. Beg, S. Chawla, J. Cobble, S. Gaillard, D. Hey, A. MacKinnon, A. MacPhee, P. Nilson, D. Offermann, S. Le Pape, and M. Schmitt, J. Phys: Conf. Ser. **244**, 022033 (2010).
[43]L. Willingale, G. M. Petrov, A. Maksimchuk, J. Davis, R. R. Freeman, T. Matsuoka, C. D. Murphy, V. M. Ovchinnikov, L. V. Woerkom, and K. Krushelnick, Plasma Phys. Control. Fusion **53**, 014011 (2011).
[44]A. Pukhov, Phys. Rev. Lett. **86**, 3562 (2001).
[45]S. Wilks, A. Langdon, T. Cowan, M. Roth, M. Singh, S. Hatchett, M. Key, D. Pennington, A. MacKinnon, and R. Snavely, Phys. Plasmas **8**, 542 (2001).
[46]Y. Sentoku, T. Cowan, A. Kemp, and H. Ruhl, Phys. Plasmas **10**, 2009 (2003).
[47]G. M. Petrov, L. Willingale, J. Davis, T. Petrova, A. Maksimchuk, and K. Krushelnick, Phys. Plasmas **17**, 103111 (2010).
[48]K. Flippo, B. Hegelich, B. Albright, L. Yin, D. Gautier, S. Letzring, M. Schollmeier, J. Schreiber, R. Schulze, and J. Fernandez, Laser Part. Beams **25**, 3 (2007).
[49]M. Roth, T. Cowan, M. Key, S. Hatchett, C. Brown, W. Fountain, J. Johnson, D. Pennington, R. Snavely, S. Wilks, K. Yasuike, H. Ruhl, F. Pegoraro, S. Bulanov, E. Campbell, M. Perry, and H. Powell, Phys. Rev. Lett. **86**, 436 (2001).
[50]E. Clark, K. Krushelnick, J. Davies, M. Zepf, M. Tatarakis, F. Beg, A. Machacek, P. Norreys, M. Santala, I. Watts, and A. Dangor, Phys. Rev. Lett. **84**, 670 (2000).
[51]M. Borghesi, A. Schiavi, D. Campbell, M. Haines, O. Willi, A. MacKinnon, L. Gizzi, M. Galimberti, R. Clarke, and H. Ruhl, Plasma Phys. Control. Fusion **43**, A267 (2001).
[52]M. Borghesi, D. Campbell, A. Schiavi, M. Haines, O. Willi, A. MacKinnon, P. Patel, L. Gizzi, M. Galimberti, R. Clarke, F. Pegoraro, H. Ruhl, and S. Bulanov, Phys. Plasmas **9**, 2214 (2002).
[53]J. Cobble, R. Johnson, T. Cowan, N. Renard-Le Galloudec, and M. Allen, J. Appl. Phys. **92**, 1775 (2002).
[54]L. Willingale, A. Thomas, P. Nilson, M. Kaluza, S. Bandyopadhyay, A. Dangor, R. Evans, P. Fernandes, M. Haines, C. Kamperidis, R. Kingham, S. Minardi, M. Notley, C. Ridgers, W. Rozmus, M. Sherlock, M. Tatarakis, M. Wei, Z. Najmudin, and K. Krushelnick, Phys. Rev. Lett. **105**, 95001 (2010).
[55]L. Willingale, P. Nilson, M. Kaluza, A. Dangor, R. Evans, P. Fernandes, M. Haines, C. Kamperidis, R. Kingham, C. Ridgers, M. Sherlock, A. Thomas, M. Wei, Z. Najmudin, K. Krushelnick, S. Bandyopadhyay, M. Notely, S. Minardi, M. Tatarakis, and W. Rozmus, Phys. Plasmas **17**, 043104 (2010).
[56]L. Willingale, P. Nilson, A. Thomas, J. Cobble, R. Craxton, A. Maksimchuk, P. Norreys, T. Sangster, R. Scott, C. Stoeckl, C. Zulick, and K. Krushelnick, Phys. Rev. Lett. **106**, 105002 (2011).
[57]M. Kaluza, J. Schreiber, M. Santala, G. Tsakiris, K. Eidmann, J. Meyer-ter Vehn, and K. Witte, Phys. Rev. Lett. **93**, 45003 (2004).
[58]A. J. Mackinnon, P. K. Patel, R. P. Town, M. J. Edwards, T. Phillips, S. C. Lerner, D. W. Price, D. Hicks, M. H. Key, S. Hatchett, S. C. Wilks, M. Borghesi, L. Romagnani, S. Kar, T. Toncian, G. Pretzler, O. Willi, M. Koenig, E. Martinolli, S. Lepape, A. Benuzzi-Mounaix, P. Audebert, J. C. Gauthier, J. King, R. Snavely, R. R. Freeman, and T. Boehlly, Rev. Sci. Instrum **75**, 3531 (2004).
[59]OMEGA EP Operations, see http://www.lle.rochester.edu/omega_facility/omega_ep/.
[60]S. Skupsky, R. Short, T. Kessler, R. Craxton, S. Letzring, and J. Soures, J. Appl. Phys. **66**, 3456 (1989).
[61]Y. Lin, T. Kessler, and G. Lawrence, Opt. Lett. **20**, 764 (1995).
[62]D. Bradley, P. Bell, J. Kilkenny, R. Hanks, O. Landen, P. Jaanimagi, P. McKenty, and C. Verdon, Rev. Sci. Instrum. **63**, 4813 (1992).
[63]Ashland Corp., see http://www.gafchromic.com/.
[64]Goodfellow Corp., see http://www.goodfellow.com/.
[65]J. Ziegler, J. Biersack, and U. Littmark, *The Stopping and Range of Ions in Matter* (Pergamon, New York, 1985).
[66]D. Hey, M. Key, A. Mackinnon, A. MacPhee, P. Patel, R. Freeman, L. Van Woerkom, and C. Castaneda, Rev. Sci. Instrum. **79**, 053501 (2008).
[67]F. H. Seguin, C. K. Li, M. J.-E. Manuel, H. G. Rinderknecht, N. Sinenian, J. A. Frenje, J. R. Rygg, D. G. Hicks, R. D. Petrasso, J. Delettrez, R. Betti, F. J. Marshall, and V. A. Smalyuk, Phys. Plasmas **19**, 012701 (2012).
[68]C. Barty, M. Key, J. Britten, R. Beach, G. Beer, C. Brown, S. Bryan, J. Caird, T. Carlson, J. Crane, J. Dawson, A. Erlandson, D. Fittinghoff, M. Hermann, C. Hoaglan, A. Iyer, L. Jones II, I. Jovanovic, A. Komashko, O. Landen, Z. Liao, W. Molander, S. Mitchell, E. Moses, N. Nielsen, H.-H. Nguyen, J. Nissen, S. Payne, D. Pennington, L. Risinger, M. Rushford, K. Skulina, M. Spaeth, B. Stuart, G. Tietbohl, and B. Wattellier, Nucl. Fusion **44**, S266 (2004).